ARTICLES
https://doi.org/10.1038/s41550-022-01677-0
nature astronomy

Check for updates

The internal rotation of the Sun and its link to the solar Li and He surface abundances

P. Eggenberger[1]✉, G. Buldgen[1], S.J.A.J. Salmon[1], A. Noels[2], N. Grevesse[2,3] and M. Asplund[4]

The Sun serves as a natural reference for the modelling of the various physical processes at work in stellar interiors. Helioseismology results, which inform us on the characterization of the interior of the Sun (such as, for example, the helium abundance in its envelope), are, however, at odds with heavy element abundances. Moreover, the solar internal rotation and surface abundance of lithium have always been challenging to explain. We present results of solar models that account for transport of angular momentum and chemicals by both hydrodynamic and magnetic instabilities. We show that these transport processes reconcile the internal rotation of the Sun, its surface lithium abundance, and the helioseismic determination of the envelope helium abundance. We also show that the efficiency of the transport of chemicals required to account for the solar surface lithium abundance also predicts the correct value of helium, independently from a specific transport process.

The internal properties of the Sun can be unravelled thanks to the study of its oscillations, named helioseismology. This has led to major successes such as the determination of the solar sound speed and density profiles, the location of the base of the convective envelope and the determination of the helium content in the convective envelope[1,2]. Standard solar models computed with the photospheric abundances available in the 90s (ref. [3]) were able to successfully reproduce all these constraints[4], so that the Sun was generally considered to be globally understood. However, the downward revision of the metallicity of the Sun by about 25% (ref. [5]) (AGSS09 hereafter) led to strong inconsistencies between standard solar models and helioseismic measurements. As a consequence of this change, the solar convective zone is too shallow, its helium surface abundance is too low and the sound speed profile is incompatible with that of the Sun[6,7]. These severe discrepancies between helioseismic constraints and solar model predictions based on the new abundances are referred to as the solar modelling problem. Besides this issue, the internal rotation of the Sun and its surface abundance of lithium have always been difficult to explain. The lithium abundance predicted by standard solar models is indeed much higher than the observed photospheric value[8]. Similarly, the nearly uniform rotation in the solar radiative zone revealed by helioseismic data cannot be reproduced by rotating models accounting solely for hydrodynamic transport processes, which predict a high degree of radial differential rotation[9–12]. This demonstrates that additional physical transport mechanisms are missing in the solar radiative interior. Magnetic fields are prime candidates for such missing processes[13]. While large-scale fossil fields can be invoked to account for the internal rotation of the Sun[14–18], key difficulties are faced in explaining the sharp transition from nearly uniform rotation in the solar radiative zone to latitudinal differential rotation in the convective envelope[19,20]. Moreover, a substantial increase of the viscosity in the solar radiative zone seems to be required in addition to a large-scale fossil magnetic field[16,18]. In this context, magnetic instabilities play an important role. In stellar radiative interiors, the Tayler instability[21] is likely to be the first magnetic instability to set in[22]. Together with the winding-up of an initially weak field by differential rotation, this instability could produce a small-scale dynamo referred to as the Tayler–Spruit dynamo[23,24]. The viability of this kind of dynamo in stellar interiors has been tested through numerical simulations leading to contrasting results[25,26]. While a definitive answer about this process is awaiting simulations performed under realistic stellar conditions[20], it has been found to explain the nearly uniform rotation in the radiative interior of the Sun and the sharp transition to differential rotation in its convective envelope[11,23,27] in the case of models computed with the old solar abundances[3]. Here we study the impact of these hydrodynamic and magnetic transport processes on solar models computed with the revised AGSS09 abundances, with a peculiar focus on the solar modelling problem and the surface abundances of light elements.

Results

We begin by studying the impact of the AGSS09 solar abundances on the internal angular-momentum transport results previously obtained with the old abundances[11,27]. We compute a one solar mass model with hydrodynamic and magnetic instabilities from the pre-main sequence to the age of the Sun by calibrating the initial chemical composition and the mixing-length parameter for convection to reproduce the solar photospheric abundances as given by AGSS09, the solar luminosity and radius after 4.57 Gyr. These solar models are computed with the Geneva stellar evolution code using OPAL opacities and equations of state[28]. Atomic diffusion is taken into account using the collision integrals of Paquette et al.[29]. The hypothesis of shellular rotation[30] is used and the transport of angular momentum and chemicals is computed simultaneously to the evolution of the star by taking into account meridional currents, shear instability and the magnetic Tayler instability. The equation describing the internal angular-momentum transport in radiative zones is then given by[28,31]

$$\rho \frac{\mathrm{d}}{\mathrm{d}t}\left(r^2\Omega\right)_{M_r} = \frac{1}{5r^2}\frac{\partial}{\partial r}\left(\rho r^4 \Omega U(r)\right) + \frac{1}{r^2}\frac{\partial}{\partial r}\left(\rho(D_{\mathrm{shear}} + \nu_{\mathrm{T}})r^4\frac{\partial \Omega}{\partial r}\right), \quad (1)$$

[1]Département d'Astronomie, Université de Genève, Versoix, Switzerland. [2]STAR Institute, Université de Liège, Liège, Belgium. [3]Centre Spatial de Liège, Université de Liège, Angleur-Liège, Belgium. [4]Australian Academy of Science, Canberra, Australian Capital Territory, Australia. ✉e-mail: patrick.eggenberger@unige.ch

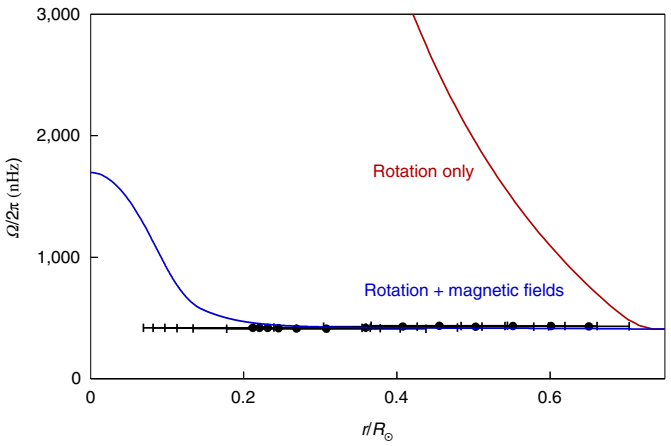

Fig. 1 | Rotation profiles in the solar radiative interior for models computed with the AGSS09 photospheric abundances. The red and blue lines correspond to solar models computed with hydrodynamic and with both hydrodynamic and magnetic instabilities, respectively. Dots indicate helioseismic measurements with their 1σ error bars[58].

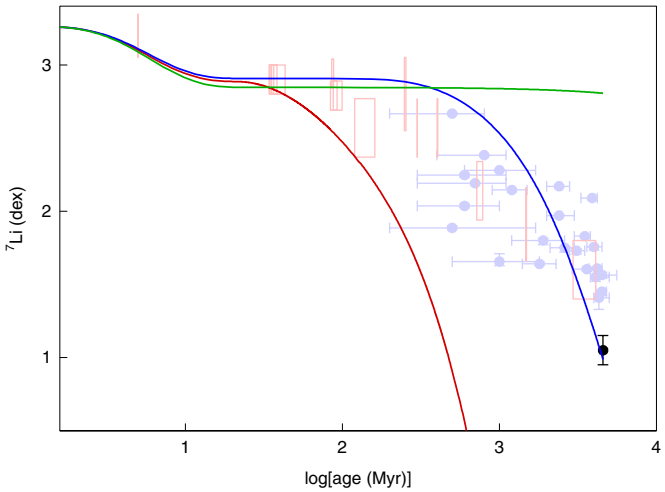

Fig. 2 | Lithium surface abundance as a function of age for different solar models. The meteoritic value of AGSS09 is used for the initial lithium abundance. The green line indicates a standard non-rotating solar model. The red line denotes a model computed with only hydrodynamic transport processes. The blue line corresponds to a model computed with hydrodynamic and magnetic transport processes. The black dot denotes the photospheric lithium abundance of the Sun with its 1σ error bars as reported by AGSS09. Orange squares indicate surface lithium abundances observed in young open clusters as given in Dumont et al.[12] and references therein. Purple dots correspond to lithium abundances observed in solar-type stars by Carlos et al.[60] with their 1σ error bars (only stars with ages lower than the solar one are shown).

with r, t, Mr, ρ and Ω, the radius, time, mass interior to radius r, mean density and mean angular velocity on an isobar, respectively. $U(r)$ denotes the radial dependence of the meridional circulation velocity in the radial direction. The expression for this velocity is given by Maeder and Zahn[32] and takes into account the role of chemical gradients and horizontal turbulence. $D_{\rm shear}$ corresponds to the diffusion coefficient for angular-momentum transport by the shear instability; the expression derived by Talon and Zahn[33] is used for the sake of consistency, because it takes into account the role of chemical gradients and horizontal turbulence as in the expression of $U(r)$ of Maeder and Zahn[32]. No free parameters are calibrated in these expressions of $U(r)$ and $D_{\rm shear}$. Horizontal turbulence is modelled by using the prescription of Maeder[34]. The uncertainty on the exact value of this coefficient is reflected in the constant n appearing in this expression; this parameter n is simply left fixed to its default value of 1 (the impact of horizontal turbulence is investigated in Methods). The quantity $\nu_{\rm T}$ corresponds to the viscosity associated with angular-momentum transport by the Tayler instability. This magnetic transport is taken into account following Spruit[23] with the viscosity

$$\nu_{\rm T} = r^2 \Omega q^2 \left(\frac{\Omega}{N_{\rm eff}}\right)^4, \qquad (2)$$

where $q = -\frac{\partial \ln \Omega}{\partial \ln r}$ and $N_{\rm eff}$ is an effective Brunt–Väisälä frequency given by

$$N^2_{\rm eff} = \frac{\eta}{K} N^2_{\rm T} + N^2_{\mu}, \qquad (3)$$

with $N_{\rm T}$ and N_{μ} the thermal and chemical composition components of the Brunt–Väisälä frequency and η and K the magnetic and thermal diffusivities. This magnetic transport is at work only when the shear parameter q is larger than a minimum threshold $q_{\rm min}$ given by

$$q_{\rm min} = \left(\frac{N_{\rm eff}}{\Omega}\right)^{7/4} \left(\frac{\eta}{r^2 N_{\rm eff}}\right)^{1/4}. \qquad (4)$$

A very efficient angular-momentum transport that leads to a flat radial rotation profile is assumed in convective zones and braking of the stellar surface by magnetized winds is taken into account following Matt et al.[35].

Regarding chemical elements, the same transport efficiency by the shear instability is taken for angular momentum and chemicals. The transport of chemicals through the simultaneous action of vertical advection and horizontal turbulence is described by the coefficient $D_{\rm eff} = |rU(r)|^2/30D_{\rm h}$ (ref. [36]), with $D_{\rm h}$ the coefficient for horizontal turbulence from Maeder[34]. Finally, the direct transport of chemical elements by the Tayler instability is given by[23]:

$$D_{\rm T} = r^2 \Omega q^4 \left(\frac{\Omega}{N_{\rm eff}}\right)^6, \qquad (5)$$

when the shear parameter q is larger than the threshold $q_{\rm min}$ given in equation (4). Within this theoretical framework, the transport of chemical elements is thus directly and self-consistently derived from the rotational and magnetic properties of the model without introducing any additional free parameter. In particular, no parameters are introduced to arbitrarily differentiate between the efficiency of transport of angular momentum and chemicals or to arbitrarily reduce the inhibiting effects of the chemical gradients as usually done in codes approximating the advective transport of angular momentum by a purely diffusive scheme[9].

A solar model including this treatment of rotational and magnetic effects is then computed with the AGSS09 solar abundances. An initial rotation rate of 5 times the present-day solar equatorial rotation rate and a disk lifetime of 6 Myr is adopted; this corresponds to a moderate rotator case that reproduces the variation with time of the 50th rotational percentile observed for solar-type stars in open clusters[27]. A corresponding solar model is computed by including only rotational effects without any magnetic transport. The rotation profiles predicted for these solar models are shown in Fig. 1. The internal rotation of the model with both hydrodynamic and magnetic transport processes (blue line in Fig. 1) results from the balance between differential rotation created by central contraction and braking of the envelope through magnetized winds and the

Table 1 | Comparison between the properties of a standard solar model and the model with hydrodynamic and magnetic instabilities

Model	A(Li) (dex)	Y_{cz}	$(r/R)_{BCZ}$
No rotation	2.81	0.2366	0.723
Rotation + magnetic	1.01	0.2463	0.728
None (observed)	1.05 ± 0.10 (ref. [5])	0.2485 ± 0.0035 (ref. [39])	0.713 ± 0.001 (ref. [43])

internal angular-momentum transport by hydrodynamic and magnetic instabilities. The magnetic Tayler instability is found to largely dominate the angular-momentum transport and leads to an internal rotation in agreement with helioseismic measurements contrary to a purely hydrodynamic model (red line in Fig. 1). This is an important result: transport by the Tayler instability still provides a physical explanation for the internal rotation of the Sun in the case of the revised AGSS09 abundances.

After angular-momentum transport, we investigate the transport of chemical elements in our models. The simultaneous impact of hydrodynamic and Tayler instabilities on chemical elements, and in particular on light elements, has not been studied for the Sun. Figure 2 shows the evolution of the lithium surface abundance for the two rotating solar models for which the rotation profiles at the age of the Sun are shown in Fig. 1. In addition to these rotating models, a standard solar model is computed without any rotational and magnetic effects (green line in Fig. 2). As illustrated by the green line in Fig. 2, a non-rotating solar model that solely accounts for atomic diffusion in stellar radiative zones is known to predict a too low lithium depletion to reproduce the solar abundance[8]. Conversely, the high degree of radial differential rotation that characterizes the purely hydrodynamic model results in a very efficient transport of chemicals by the shear instability that leads to the complete depletion of lithium (red line in Fig. 2). Such a model is thus unable to account either for the internal rotation or lithium abundance of the Sun and is consequently not considered anymore in the following discussion. The transport of chemical elements in the model computed with both rotational and magnetic effects results from the simultaneous action of atomic diffusion and hydrodynamic and the magnetic Tayler instabilities. The main properties of this model and of the standard non-rotating model are given in Table 1 (more details are provided in Supplementary Table 1). Accounting for both hydrodynamic and magnetic instabilities enables us to reproduce the photospheric solar value (blue line in Fig. 2). This is a key result: the efficient angular-momentum transport imposed by the magnetic Tayler instability leads simultaneously to an internal rotation in accordance with helioseismic constraints and a transport of chemicals (mainly through the combined action of atomic diffusion and shear instability) that is able to account for the solar lithium depletion. The same physical explanation is then able to account for these two fundamental solar constraints without any need of another transport process nor fine-tuning of free parameters (see the discussion about the modelling of transport processes in the first section of Methods).

To put this result somewhat in perspective, we briefly compare it with the most recent parametric study of transport processes in solar-type stars[12]. While the latter study has quantified the efficiency of the missing angular-momentum transport process by introducing a constant additional viscosity, we here propose a physical explanation for this missing process. The need for two additional and distinct parametric mixing processes (one for angular momentum and one for chemical elements) has also been suggested to

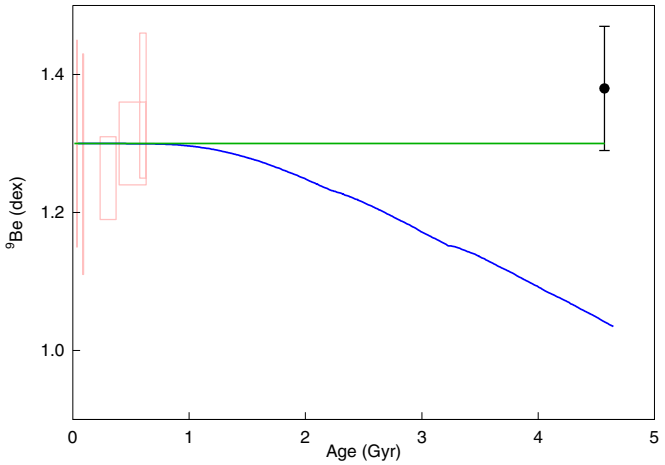

Fig. 3 | Beryllium surface abundance as a function of age for different solar models. The green line indicates the standard non-rotating solar model and the blue line the model with hydrodynamic and magnetic instabilities. The meteoritic AGSS09 abundance is adopted for the initial beryllium abundance. The black dot indicates the photospheric AGSS09 determination of the solar abundance with its 1σ error bars. Orange squares indicate surface beryllium abundances observed in young open clusters as given in Dumont et al.[12] and references therein.

simultaneously explain the internal rotation and the lithium abundance of the Sun[12]. Our results deliver an interesting new picture: once a coherent physical description of hydrodynamic and magnetic instabilities is implemented, an internal rotation in agreement with solar constraints is obtained that naturally leads to the observed depletion of lithium in the Sun.

The variation with time of the beryllium surface abundance is shown in Fig. 3 for the same solar models. The model with rotational and magnetic effects also predicts a slight depletion of beryllium that is not favoured by current observations. However, as suggested by Asplund et al.[37], revisiting the solar beryllium abundance with three-dimensional non-local thermodynamic equilibrium calculations would be worthwhile. Furthermore, unaccounted blends might have biased the inferred beryllium abundance upward. Obtaining a reliable determination of surface beryllium abundance for the Sun would be particularly useful as an additional test of our models with rotation and magnetic fields.

A key issue for standard solar models computed with the abundances of AGSS09 is their inability to reproduce the helium mass fraction in the convective zone determined from helioseismology[6,7,38]. Indeed, these standard solar models exhibit a lower value, incompatible with helioseismic constraints (typically a mass fraction of about 0.237, compared with the value of 0.2485 ± 0.0035 from Basu and Antia[39]), as illustrated by the green line in Fig. 4, where we show the variation of surface helium with time for our various solar models. The model computed with both hydrodynamic and magnetic instabilities predicts a solar helium mass fraction in agreement with the helioseismic value (blue line in Fig. 4). This model is thus able to simultaneously reproduce the variation with time of surface rotation velocities observed in open clusters[27], the internal rotation of the Sun as deduced from helioseismic data (Fig. 1), the solar lithium depletion (Fig. 2) and the helioseismic determination of the helium abundance in the convective envelope (Fig. 4). In addition to its effect on the helium abundance, the additional mixing also reduces the variation between the initial and present-day metal abundances with a typical difference of about 0.03 dex. This leads to a new view on solar models: reproducing the internal rotation of the Sun or its lithium abundance has usually

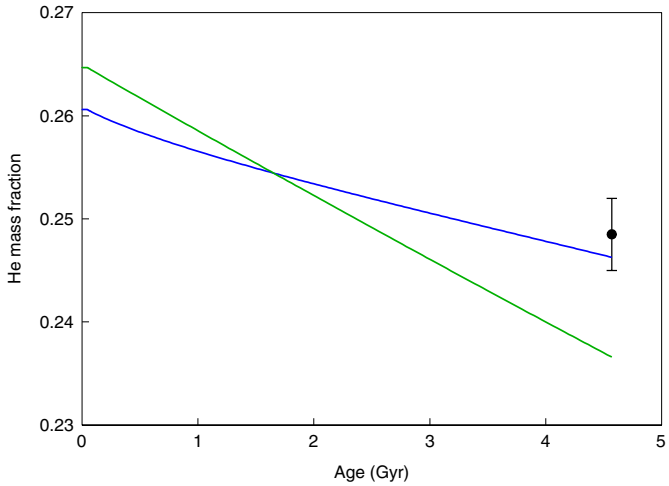

Fig. 4 | Evolution of the surface helium mass fraction as a function of age for different solar models. The green line indicates the standard non-rotating solar model and the blue line the model with hydrodynamic and magnetic instabilities. The black dot indicates the helioseismic determination of the surface helium mass fraction of the Sun with its 1σ error bars from Basu and Antia[39].

been seen as being somewhat disconnected from their calibration. Our results show that standard solar models are not sufficient to address the solar modelling problem given the impact of rotational and magnetic transport processes on the solar calibration procedure (in particular on the helium abundance).

We then study the impact of rotation and magnetic fields on the internal structure of the Sun as revealed by helioseismology. Figure 5 shows the inversion of the squared adiabatic sound speed for the solar model with transport by hydrodynamic and magnetic instabilities compared with the standard model. The inversions have been computed using the Substractive Optimally Localized Averages (SOLA) method[40] as in Buldgen et al.[41]. We find that the inclusion of the effects of hydrodynamic and magnetic instabilities does not substantially change the sound speed profile. The same conclusion is reached from the comparison of the frequency ratios of low-degree p-modes (Supplementary Fig. 2). Reproducing the internal rotation of the Sun with transport by hydrodynamic and magnetic instabilities is thus found to provide a natural solution to the solar modelling problem related to helium and lithium abundances, while another contribution (coming for instance from micro-physics) is needed to solve the part of the problem related to structural inversion results.

We finally investigate whether the link found between lithium and helium abundances for solar models with the AGSS09 abundances that accounts for rotational and magnetic effects is more general and could be obtained independently from the specific physical transport processes considered. To this aim, we simply compute non-rotating solar models that include an arbitrary parametric coefficient for the transport of chemicals in the radiative zone. This parametric coefficient is taken as a constant C times the ratio of the density at the base of the convective zone to the density of the considered layer to a power n (ref. [8]). This simple parametric coefficient does not rely on any physical ground and the choice of the values of C and n to account for the lithium abundance of the Sun is of course not unique. A value of $n=3$ is first adopted with a constant $C=7{,}500$, while another solar model is computed for lower values of the constant $C=2{,}900$ and the exponent $n=1.3$. This case corresponds to a lower transport efficiency at the bottom of the convective zone compared with the previous model, but with a smoother decrease in the amplitude of the coefficient when the radius decreases (Supplementary Fig. 3). In addition to these models computed with the AGSS09 abundances, another model is computed by accounting for the recent revised solar neon and lithium abundances from Asplund et al.[37] and Wang et al.[42], respectively. Finally, we compute a model with an overshooting at the base of the convective envelope calibrated to correctly reproduce the helioseismic determination of the location of the base of the convective envelope of the Sun of 0.713 ± 0.001 solar radius[43]. The temperature gradient is extended adiabatically in the overshooting region and an overshooting of $0.17\,H_p$ (with Hp the pressure scale height) is found. As a consequence of overshooting, a higher pre-main-sequence lithium depletion is observed for this model (in contradiction with lithium abundances for solar-type stars younger than the Sun, as shown by the light-blue line in Fig. 6), and a lower value of $C=1{,}300$ is then determined for $n=1.3$ to account for the solar lithium content.

The evolution of the surface lithium and helium abundances of these parametric models is shown in Figs. 6 and 7, respectively, while their properties are given in Supplementary Table 1. For the sake of completeness, the evolution of the surface beryllium for these models is shown in Supplementary Fig. 4 and the inversion of the sound speed profile is shown in Supplementary Fig. 5 for the model with the recent revised neon abundance from Asplund et al.[37] and for the one with overshooting. Despite the very different shapes of the coefficients, we find that the solar helium abundance is globally compatible with the helioseismic value of Basu and Antia[39] for these models (although generally in the low range) once the parametric diffusion coefficient is calibrated to reproduce the solar lithium abundance. This shows that the efficiency of mixing needed to account for the solar lithium depletion is able to counteract the gravitational settling of helium to lead to a surface helium abundance at the solar age in accordance with helioseismic constraints. This result reveals interesting new properties of solar models with the revised AGSS09 abundances, since a parametric study of rotational mixing aiming at reproducing the surface lithium abundance for models with the old solar abundances concluded that only a negligible increase in the solar helium abundance was then obtained[44]. More importantly, this reconciles the helioseismic constraint on the helium abundance with the revised solar abundances of AGSS09. We also find that the

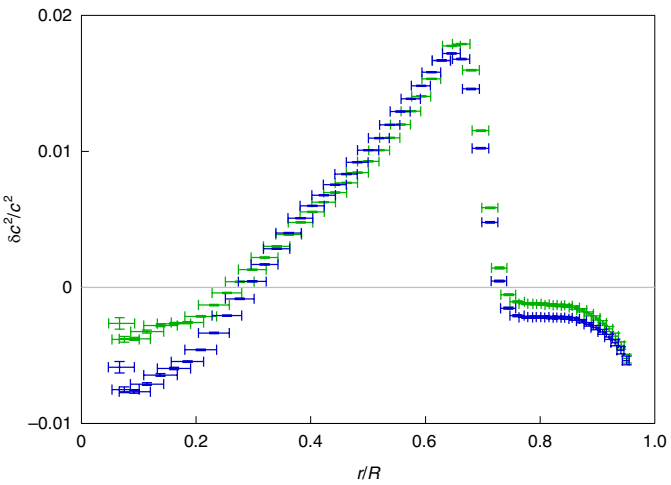

Fig. 5 | Relative differences in the squared adiabatic sound speed c^2 between the Sun and solar models obtained by inversion. The green dots indicate the standard solar model, while the blue dots correspond to the model computed with hydrodynamic and magnetic instabilities. Horizontal error bars show the interquartile width of the averaging kernels while the vertical error bars are the 1σ errors from the propagation of the observational 1σ errors.

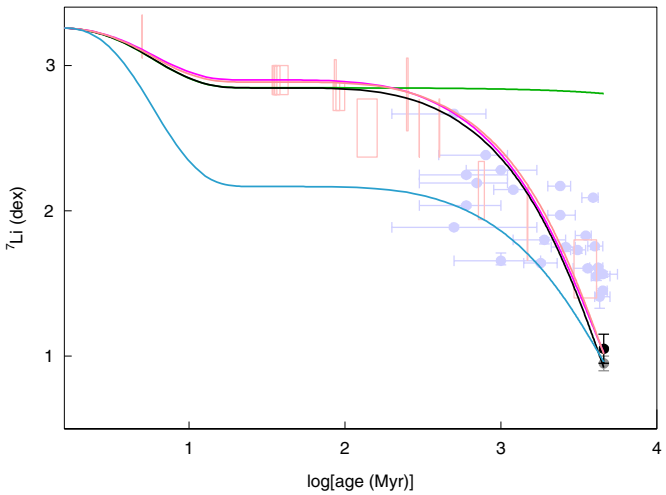

Fig. 6 | Lithium surface abundance as a function of age for the different non-rotating solar models. All lines correspond to models with the AGSS09 abundances except the black line that denotes a model with a higher neon abundance as derived by Asplund et al.[37]. The green, magenta, orange and black lines correspond to models without overshooting, while the light-blue line corresponds to a model with an overshooting below the convective envelope of 0.17 H_p. The orange and magenta lines are partly superimposed. The green line indicates a standard solar model. The magenta, orange, light-blue and black lines indicate non-rotating models computed with a parametric turbulent diffusion coefficient with values of $C=7{,}500$, $n=3$; $C=2{,}900$, $n=1.3$; $C=1{,}300$, $n=1.3$; and $C=3{,}000$, $n=1.3$, respectively. The meteoritic value of AGSS09 is used for the initial lithium abundance. The black and grey dots denote the photospheric surface lithium abundance of the Sun with their 1σ error bars reported by AGSS09 and Wang et al.[42], respectively. Orange squares indicate surface lithium abundances observed in young open clusters as given in Dumont et al.[12] and references therein. Purple dots correspond to lithium abundances observed in solar-type stars by Carlos et al.[60] (only stars with ages lower than the solar one are shown).

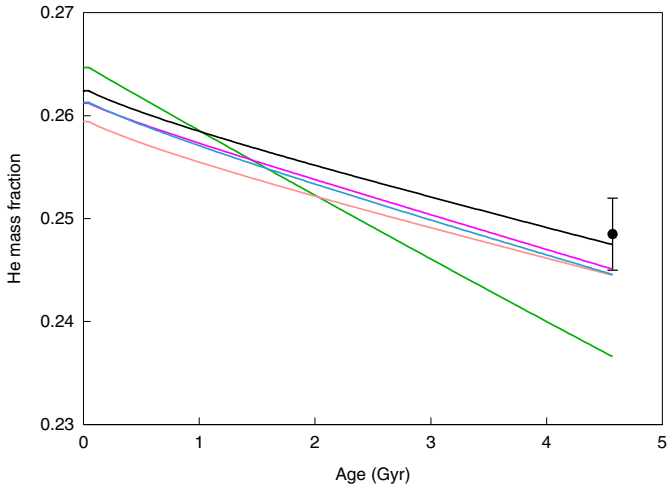

Fig. 7 | Evolution of the surface helium mass fraction as a function of age for non-rotating solar models. The colours of the different lines correspond to the same models as in Fig. 6. The black dot indicates the helioseismic determination of the surface helium mass fraction of the Sun with its 1σ error bars by Basu and Antia[39].

capability of solar models with AGSS09 abundances to simultaneously account for the lithium and helium photospheric abundances is not affected by the inclusion of overshooting to reproduce the location of the base of the convective envelope of the Sun.

Discussion

Once a coherent physical description of hydrodynamic and magnetic instabilities is accounted for in solar models with AGSS09 abundances, an internal rotation in agreement with helioseismic constraints is obtained that naturally leads to the observed depletion of lithium and the helioseismically inferred surface helium abundance. This provides for the first time a physical explanation for the solar modelling problem related to the surface helium abundance, while simultaneously explaining the solar rotation profile and surface lithium abundance.

In addition to the Sun, these results are of key interest for main-sequence low-mass stars in general, for which a similar efficient angular-momentum transport in radiative interiors is favoured by asteroseismic measurements[45,46]. While this is particularly encouraging for our understanding of angular momentum in main-sequence stars, we however note that we are still far from having a global understanding of angular-momentum transport in stars at different evolutionary stages, since no physical explanation is currently available to reproduce the internal rotation of evolved stars[47–49]. Moreover, we focus here on the impact of the Tayler magnetic instability on the transport in radiative zones; it would be of prime interest to also consider the impact of magnetic fields on convection in the context of the solar modelling problem[50]. Other processes could also play an important role for angular-momentum transport in stellar interiors; it would be particularly valuable to study the agreement of models accounting for transport by internal gravity waves[10,51] with the internal rotation and surface helium abundance of the Sun as deduced from helioseismic data.

We find that the link between the solar lithium and helium abundances is independent from the specific physical process considered for the transport of chemicals. This reconciles the helioseismic constraint on the helium content of the solar convective envelope with the predictions of models with AGSS09 abundances. This finding also underlines the need to account for dynamical transport processes in the solar calibration procedure. We are of course still far from solving the solar modelling problem as a whole, since models with rotational and magnetic effects still predict too shallow convective envelopes and sound speed profiles that are not in better agreement with helioseismic data than standard models. A revision of radiative opacities close to the base of the convective envelope could be the secondary actor in solving the solar problem[41,52,53]. Such local altering of the temperature gradient would then be able to significantly improve the agreement in both sound speed and position of the base of the convective zone, and would thus be complementary to our solution related to rotational and magnetic effects. As noted above and as known from the literature, a full answer to the solar modelling problem also requires improvements to microphysical ingredients of solar models.

Methods

Impact of uncertainties in the modelling of transport processes. The main uncertainty in the computation of the present models with rotational and magnetic effects comes from the modelling of horizontal turbulence. This is taken into account in the prescription for horizontal turbulence in Maeder[34] by introducing a parameter n that can differ from 1 with values between 1 and 5 (equation (19) in Maeder[34]). The results presented in the main text have been obtained by simply letting n be fixed to 1. We here investigate the impact of this uncertainty on our results by computing an additional solar model with $n=5$ instead of 1 in the prescription of Maeder[34].

The change in the modelling of horizontal turbulence has no effect on the transport of angular momentum in solar models with hydrodynamic and magnetic instabilities. As a result, the same rotation profile as the one shown by the blue line in Fig. 1 is predicted for the Sun with $n=5$ instead of 1 in the horizontal turbulence prescription of Maeder[34]. This is of course not surprising: comparing the red and

blue lines in Fig. 1 clearly shows that angular-momentum transport is largely dominated by magnetic effects. A change in the hydrodynamic transport therefore has no consequences on the solar rotation profile predicted by these models. We also recall that no free parameters are introduced in the modelling of magnetic effects. The predicted solar rotation profile directly follows from the physics of the Tayler–Spruit dynamo and in particular from the condition for this process to operate (equation (4)) and the associated effective viscosity (equation (2)). This also explains why almost identical rotation profiles are obtained at the solar age for very different initial rotational velocities or disk lifetimes[27]. The fact that this predicted internal rotation is in good agreement with the solar rotation profile deduced from helioseismic data therefore constitutes a strong point for the Tayler–Spruit dynamo.

While the transport of angular momentum in these models is not impacted by uncertainties related to hydrodynamic processes, the situation is different for the transport of chemical elements. Indeed, the transport of chemicals implies an additional source of complexity compared with angular-momentum transport, which is simply related to the amount of chemical mixing predicted for a given rotation profile. Consequently, uncertainties in the modelling of hydrodynamic processes can more easily affect the transport of chemical elements. This is illustrated in Supplementary Fig. 1 with a comparison between the evolution of surface lithium and helium abundances for solar models computed with different values for the horizontal turbulence ($n=1$ and 5 in the horizontal turbulence prescription of Maeder[34] shown by the continuous and dotted lines, respectively). The model with $n=5$ shows a higher solar surface lithium abundance than the corresponding model with $n=1$, while only a negligible decrease in the surface helium abundance is obtained at the solar age. Contrary to angular-momentum transport, the shear instability is found to largely dominate the transport of chemical elements in models with hydrodynamic and magnetic instabilities with only a negligible direct transport by the Tayler instability. We thus obtain the following global picture: the Tayler instability regulates internal angular-momentum transport and imposes the degree of radial differential rotation that then leads to transport of chemical elements by the shear instability. Recalling that horizontal turbulence enables partially overcoming the inhibiting effects of stratification on transport by the shear instability (in particular, the strong inhibiting effects of chemical gradients)[33], a lower mixing efficiency is expected when the horizontal turbulence is decreased. This explains why the model with a higher value of n, which corresponds to a lower value for the coefficient of horizontal turbulence, is characterized by a lower mixing efficiency and hence a lower depletion of lithium at the solar age. Supplementary Figure 1 enables us to evaluate somewhat the impact of the uncertainties regarding the modelling of transport processes within our theoretical framework on the predicted surface abundances. We see that these uncertainties have no major impact on the results; to precisely reproduce the solar lithium abundance, a decrease in the efficiency of horizontal turbulence as prescribed by Maeder[34] is simply disfavoured, while a negligible impact is observed on the predicted solar surface helium abundance, which is always correctly reproduced.

Finally, we discuss the prescriptions adopted for the different transport processes. As noted above, horizontal turbulence is modelled according to Maeder[34]. This prescription is derived theoretically by considering the dissipation of energy in the horizontal shear. Another prescription has been obtained by Mathis et al.[54] based on experimental results obtained by Richard and Zahn[55]. As discussed in Maeder[34] and Mathis et al.[54], both prescriptions are preferred over the original formulation of Zahn[30], which corresponds to an estimate of the minimal value needed for horizontal turbulence for the shellular rotation hypothesis to remain valid rather than to a detailed prescription. Interestingly, while derived from different considerations, both prescriptions lead to very similar values for the coefficient of horizontal turbulence[54]. Consequently, the use of the Mathis et al.[54] prescription for horizontal turbulence instead of the Maeder[34] one has no substantial impact on our results. The modelling of transport by the shear instability is based on the expression derived by Talon and Zahn[33]. As mentioned in the main text, this expression accounts for the effects of chemical gradients and horizontal turbulence in the same way as in the formulation of the meridional circulation velocity by Maeder and Zahn[32]. The original prescription by Zahn[30] for the shear instability cannot be used in this context, since it does not take into account the role of horizontal turbulence nor the effects of chemical gradients. In the same way, the prescription of Mathis et al.[56] does not take into account the strong inhibiting effects of chemical gradients. Both expressions are thus only valid in layers where chemical gradients are absent, which of course cannot be applied to the present solar models, where chemical gradients built by atomic diffusion or nuclear reactions are present close to the border of the convective envelope and in the core, respectively.

Global properties and calibration parameters of the solar models. The calibration parameters and the global properties at the solar age are given in Supplementary Table 1 for the different solar models. Y_0 and Z_0 indicate the initial helium mass fraction and heavy element mass fraction of these models, respectively. $A(\mathrm{Li})$, Y_{CZ} and $(r/R)_{\mathrm{BCZ}}$ correspond to the surface lithium abundance, surface helium mass fraction and location of the base of the convective envelope at the solar age, respectively.

Frequency ratios of low-degree p-modes. In addition to the sound speed profiles, the frequency ratios of low-degree p-modes are compared for the standard non-rotating model and the model with transport by hydrodynamic and magnetic instabilities. These ratios, which are sensitive to the properties of the core, are shown in Supplementary Fig. 2. No substantial differences are seen between the standard solar model and the one with rotational and magnetic effects. This is not surprising, as Fig. 5 already shows only minor changes in sound speed between the standard non-rotating model and the one including hydrodynamic and magnetic instabilities. As the frequency ratios are a proxy of the sound speed gradient, only minor differences resulting from the deviations below $0.2\,R_\odot$ can be expected. The model including hydrodynamic and magnetic instabilities has the advantage of improving the agreement in helium and lithium abundances and reproducing the solar internal rotation profile while not leading to much larger inconsistencies in other seismic constraints.

Computation of non-rotating parametric solar models. Simple non-rotating solar models are computed by including a parametric diffusion coefficient for the transport of chemicals in radiative zones based on the work by Proffitt and Michaud[8]. This coefficient is then taken as

$$D_{\mathrm{tot}} = C\left(\frac{\rho_{\mathrm{BCZ}}}{\rho(r)}\right)^n, \tag{6}$$

with ρ_{BCZ} the density at the base of the convective envelope, while C and n are calibration parameters.

A comparison between the total diffusion coefficient of chemicals obtained from a model with hydrodynamic and magnetic instabilities and these parametric coefficients is shown in Supplementary Fig. 3. This global diffusion coefficient includes the transport of chemicals by the shear instability, meridional currents and the magnetic Tayler instability. The comparison shown in Supplementary Fig. 3 is done at the age of 2 Gyr and at the solar age. The slope of the diffusion coefficient of the model computed with $n=1.3$ is found to be similar in the external part of the radiative zone to the variation predicted by the model with the full treatment of rotational and magnetic effects. The model with $n=3$ shows a more rapid decrease in the amplitude of the coefficient when the radius decreases compared with these models.

Beryllium surface abundances of non-rotating models. The variation with time of the beryllium surface abundance is shown in Supplementary Fig. 4 for the non-rotating solar models. All models able to reproduce the solar lithium abundance also show a slight depletion of beryllium that is not favoured by current observations. However, as discussed by Asplund et al.[37], the present value of the solar abundance of beryllium might be somewhat overestimated. The solar model computed with overshooting (light-blue line in Supplementary Fig. 4) predicts a lower depletion of beryllium than models without overshooting. This results directly from the slightly lower mixing efficiency needed in the case of overshooting models to account for the solar lithium abundance. However, as discussed in the main text, this model with overshooting is inconsistent with observations of lithium abundances in young solar-type stars. The parametric solar model computed with $n=3$ (magenta line in Supplementary Fig. 4) is also characterized by a higher beryllium abundance than the corresponding model computed with $n=1.3$ (orange line in Supplementary Fig. 4). This directly reflects the different shapes of the diffusion coefficients shown in Supplementary Fig. 3.

Sound speed profiles of non-rotating models. Supplementary Figure 5 shows the inversion of the squared adiabatic sound speed for different non-rotating solar models. The inversions have been computed using the Substractive Optimally Localized Averages method[40] as in Buldgen et al.[41]. As is well known, a solar model computed with overshooting to correctly reproduce the location of the base of the convective envelope (light-blue dots in Supplementary Fig. 5) leads to a sound speed profile in better agreement with helioseismic data[38]. This is also the case for the model computed with the revised solar neon abundance of Asplund et al.[37], as a result of the related higher opacity close to the base of the convective envelope where neon is the third contributor[57].

Data availability

The solar lithium abundances used in this paper are publicly available in the papers by Asplund et al.[5] and Wang et al.[42]. The beryllium abundance is publicly available in the paper by Asplund et al.[5]. The solar inverted rotation profile shown in Fig. 1 is available in the paper by Couvidat et al.[58]. The Global Oscillations at Low Frequencies (GOLF) dataset used for the frequency ratios is publicly available from Salabert et al.[59]. The dataset used for the sound speed inversions is publicly available from the Birmingham Solar Oscillation Network (BiSON) network website (http://bison.ph.bham.ac.uk/portal/frequencies) and the Joint Science Operations Center portal (http://jsoc.stanford.edu/MDI/MDI_Global.html). All data obtained within this paper are available from the corresponding author upon reasonable request.

Code availability

The Geneva stellar evolution code is a proprietary software, but all solar evolution models will be made available upon request. The software used to compute the

sound speed inversions is publicly available on the following SpaceInn webpage: http://www.spaceinn.eu/data-access/analysis-tools-for-solar-like-oscillators/inversionkit/.

Received: 21 April 2021; Accepted: 1 April 2022;
Published online: 26 May 2022

References

1. Buldgen, G., Salmon, S. & Noels, A. Progress in global helioseismology: a new light on the solar modelling problem and its implications for solar-like stars. *Front. Astron. Space Sci.* **6**, 42 (2019).
2. Christensen-Dalsgaard, J. Solar structure and evolution. *Living Rev. Sol. Phys.* **18**, 2 (2021).
3. Grevesse, N. & Noels, A. Cosmic abundances of the elements. In *International Symposium on Origin and Evolution of the Elements* (eds Prantzos, N. et al.) 15-25 (Cambridge Univ. Press, 1993).
4. Christensen-Dalsgaard, J. et al. The current state of solar modeling. *Science* **272**, 1286-1292 (1996).
5. Asplund, M., Grevesse, N., Sauval, A. J. & Scott, P. The chemical composition of the Sun. *Ann. Rev. Astron. Astrophys.* **47**, 481 (2009).
6. Basu, S. & Antia, H. M. Helioseismology and solar abundances. *Phys. Rep.* **457**, 217-283 (2008).
7. Serenelli, A. M., Basu, S., Ferguson, J. W. & Asplund, M. New solar composition: the problem with solar models revisited. *Astrophys. J.* **705**, L123 (2009).
8. Proffitt, C. R. & Michaud, G. Gravitational settling in solar models. *Astrophys. J.* **380**, 238-250 (1991).
9. Pinsonneault, M. H., Kawaler, S. D., Sofia, S. & Demarque, P. Evolutionary models of the rotating sun. *Astrophys. J.* **338**, 424-452 (1989).
10. Charbonnel, C. & Talon, S. Influence of gravity waves on the internal rotation and Li abundance of solar-type stars. *Science* **309**, 2189-2191 (2005).
11. Eggenberger, P., Maeder, A. & Meynet, G. Stellar evolution with rotation and magnetic fields. IV. The solar rotation profile. *Astron. Astrophys.* **440**, L9 (2005).
12. Dumont, T. et al. Lithium depletion and angular momentum transport in solar-type stars. *Astron. Astrophys.* **646**, A48 (2021).
13. Mestel, L. Rotation and stellar evolution. *Mon. Not. R. Astron. Soc.* **113**, 716-745 (1953).
14. Mestel, L. & Weiss, N. O. Magnetic fields and non-uniform rotation in stellar radiative zones. *Mon. Not. R. Astron. Soc.* **226**, 123-135 (1987).
15. Charbonneau, P. & MacGregor, K. B. Angular momentum transport in magnetized stellar radiative zones. II. The solar spin-down. *Astrophys. J.* **417**, 762-780 (1993).
16. Rüdiger, G. & Kitchatinov, L. L. The internal solar rotation in its spin-down history. *Astrophys. J.* **466**, 1078-1086 (1996).
17. Gough, D. O. & McIntyre, M. E. Inevitability of a magnetic field in the Sun's radiative interior. *Nature* **394**, 755-757 (1998).
18. Spada, F., Lanzafame, A. C. & Lanza, A. F. A semi-analytic approach to angular momentum transport in stellar radiative interiors. *Mon. Not. R. Astron. Soc.* **404**, 641-660 (2010).
19. Brun, A. S. & Zahn, J.-P. Magnetic confinement of the solar tachocline. *Astron. Astrophys.* **457**, 665-674 (2006).
20. Braithwaite, J. & Spruit, H. C. Magnetic fields in non-convective regions of stars. *R. Soc. Open Sci.* **4**, 160271 (2017).
21. Tayler, R. J. The adiabatic stability of stars containing magnetic fields. I. Toroidal fields. *Mon. Not. R. Astron. Soc.* **161**, 365-380 (1973).
22. Spruit, H. C. Differential rotation and magnetic fields in stellar interiors. *Astron. Astrophys.* **349**, 189-202 (1999).
23. Spruit, H. C. Dynamo action by differential rotation in a stably stratified stellar interior. *Astron. Astrophys.* **381**, 923-932 (2002).
24. Fuller, J., Piro, A. L. & Jermyn, A. S. Slowing the spins of stellar cores. *Mon. Not. R. Astron. Soc.* **485**, 3661-3680 (2019).
25. Braithwaite, J. A differential rotation driven dynamo in a stably stratified star. *Astron. Astrophys.* **449**, 451-460 (2006).
26. Zahn, J., Brun, A. S. & Mathis, S. On magnetic instabilities and dynamo action in stellar radiation zones. *Astron. Astrophys.* **474**, 145-154 (2007).
27. Eggenberger, P., Buldgen, G. & Salmon, S. J. A. J. Rotation rate of the solar core as a key constraint to magnetic angular momentum transport in stellar interiors. *Astron. Astrophys.* **626**, L1 (2019).
28. Eggenberger, P. et al. The Geneva stellar evolution code. *Astrophys. Space Sci.* **316**, 43-54 (2008).
29. Paquette, C., Pelletier, C., Fontaine, G. & Michaud, G. Diffusion coefficients for stellar plasmas. *Astrophys. J. Suppl.* **61**, 177-195 (1986).
30. Zahn, J.-P. Circulation and turbulence in rotating stars. *Astron. Astrophys.* **265**, 115-132 (1992).
31. Mathis, S. & Zahn, J. P. Transport and mixing in the radiation zones of rotating stars. I. Hydrodynamical processes. *Astron. Astrophys.* **425**, 229-242 (2004).
32. Maeder, A. & Zahn, J.-P. Stellar evolution with rotation. III. Meridional circulation with μ-gradients and non-stationarity. *Astron. Astrophys.* **334**, 1000-1006 (1998).
33. Talon, S. & Zahn, J. P. Anisotropic diffusion and shear instabilities. *Astron. Astrophys.* **317**, 749-751 (1997).
34. Maeder, A. Stellar rotation: evidence for a large horizontal turbulence and its effects on evolution. *Astron. Astrophys.* **399**, 263-269 (2003).
35. Matt, S. P., Brun, A. S., Baraffe, I., Bouvier, J. & Chabrier, G. The mass-dependence of angular momentum evolution in Sun-like stars. *Astrophys. J.* **799**, L23 (2015).
36. Chaboyer, B. & Zahn, J.-P. Effect of horizontal turbulent diffusion on transport by meridional circulation. *Astron. Astrophys.* **253**, 173-177 (1992).
37. Asplund, M., Amarsi, A. M. & Grevesse, N. The chemical make-up of the Sun: a 2020 vision. *Astron. Astrophys.* **653**, A141 (2021).
38. Montalban, J., Miglio, A., Theado, S., Noels, A. & Grevesse, N. The new solar abundances—Part II: the crisis and possible solutions. *Commun. Asteroseismol.* **147**, 80-84 (2006).
39. Basu, S. & Antia, H. M. Helium abundance in the solar envelope. *Mon. Not. R. Astron. Soc.* **276**, 1402-1408 (1995).
40. Pijpers, F. P. & Thompson, M. J. The SOLA method for helioseismic inversion. *Astron. Astrophys.* **281**, 231-240 (1994).
41. Buldgen, G. et al. Combining multiple structural inversions to constrain the solar modelling problem. *Astron. Astrophys.* **621**, A33 (2019).
42. Wang, E. X. et al. 3D NLTE spectral line formation of lithium in late-type stars. *Mon. Not. R. Astron. Soc.* **500**, 2159-2176 (2021).
43. Basu, S. & Antia, H. M. Seismic measurement of the depth of the solar convection zone. *Mon. Not. R. Astron. Soc.* **287**, 189-198 (1997).
44. Richard, O., Vauclair, S., Charbonnel, C. & Dziembowski, W. A. New solar models including helioseismological constraints and light-element depletion. *Astron. Astrophys.* **312**, 1000-1011 (1996).
45. Benomar, O., Takata, M., Shibahashi, H., Ceillier, T. & García, R. A. Nearly uniform internal rotation of solar-like main-sequence stars revealed by space-based asteroseismology and spectroscopic measurements. *Mon. Not. R. Astron. Soc.* **452**, 2654-2674 (2015).
46. Nielsen, M. B., Schunker, H., Gizon, L. & Ball, W. H. Constraining differential rotation of Sun-like stars from asteroseismic and starspot rotation periods. *Astron. Astrophys.* **582**, A10 (2015).
47. Cantiello, M., Mankovich, C., Bildsten, L., Christensen-Dalsgaard, J. & Paxton, B. Angular momentum transport within evolved low-mass stars. *Astrophys. J.* **788**, 93 (2014).
48. Eggenberger, P. et al. Asteroseismology of evolved stars to constrain the internal transport of angular momentum. II. Test of a revised prescription for transport by the Tayler instability. *Astron. Astrophys.* **631**, L6 (2019).
49. den Hartogh, J. W., Eggenberger, P. & Deheuvels, S. Asteroseismology of evolved stars to constrain the internal transport of angular momentum. III. Using the rotation rates of intermediate-mass stars to test the Fuller-formalism. *Astron. Astrophys.* **634**, L16 (2020).
50. Feiden, G. A. & Chaboyer, B. Magnetic inhibition of convection and the fundamental properties of low-mass stars. I. Stars with a radiative core. *Astrophys. J.* **779**, 183 (2013).
51. Pinçon, C., Belkacem, K., Goupil, M. J. & Marques, J. P. Can plume-induced internal gravity waves regulate the core rotation of subgiant stars? *Astron. Astrophys.* **605**, A31 (2017).
52. Christensen-Dalsgaard, J. & Houdek, G. Prospects for asteroseismology. *Astrophys. Space Sci.* **328**, 51-66 (2010).
53. Ayukov, S. V. & Baturin, V. A. Low-Z solar model: sound speed profile under the convection zone. *J. Phys. Conf. Ser.* **271**, 012033 (2011).
54. Mathis, S., Palacios, A. & Zahn, J.-P. On shear-induced turbulence in rotating stars. *Astron. Astrophys.* **425**, 243-247 (2004).
55. Richard, D. & Zahn, J.-P. Turbulence in differentially rotating flows. What can be learned from the Couette–Taylor experiment. *Astron. Astrophys.* **347**, 734-738 (1999).
56. Mathis, S. et al. Anisotropic turbulent transport in stably stratified rotating stellar radiation zones. *Astron. Astrophys.* **620**, A22 (2018).
57. Blancard, C., Cossé, P. & Faussurier, G. Solar mixture opacity calculations using detailed configuration and level accounting treatments. *Astrophys. J.* **745**, 10 (2012).
58. Couvidat, S. et al. The rotation of the deep solar layers. *Astrophys. J.* **597**, L77 (2003).
59. Salabert, D., García, R. A. & Turck-Chièze, S. Seismic sensitivity to sub-surface solar activity from 18 yr of GOLF/SoHO observations. *Astron. Astrophys.* **578**, A137 (2015).
60. Carlos, M. et al. The Li-age correlation: the Sun is unusually Li deficient for its age. *Mon. Not. R. Astron. Soc.* **485**, 4052-4059 (2019).

Acknowledgements

We thank T. Dumont and C. Charbonnel for providing us with their compilation of observations of lithium and beryllium abundances available for solar-type stars. P.E. and S.J.A.J.S. have received funding from the European Research Council under the

European Union's Horizon 2020 research and innovation programme (grant agreement No 833925, project STAREX). G.B. acknowledges fundings from the SNF AMBIZIONE grant No 185805 (Seismic inversions and modelling of transport processes in stars).

Author contributions

P.E. led the project with the help from G.B. P.E. computed the models with the Geneva code and G.B. computed the inversions. P.E., G.B., S.J.A.J.S. and A.N. interpreted the data regarding helioseismic constraints and input physics of solar models. N.G. and M.A. interpreted the results in the context of solar spectroscopic abundance determinations. All authors have contributed to the discussion of the results and to the writing of the paper.

Competing interests

The authors declare no competing interests.

Additional information

Supplementary information The online version contains supplementary material available at https://doi.org/10.1038/s41550-022-01677-0.

Correspondence and requests for materials should be addressed to P. Eggenberger.

Peer review information *Nature Astronomy* thanks Ana Palacios, Alessandro Lanzafame and the other, anonymous, reviewer(s) for their contribution to the peer review of this work.

Reprints and permissions information is available at www.nature.com/reprints.

Publisher's note Springer Nature remains neutral with regard to jurisdictional claims in published maps and institutional affiliations.